6 Marked point processes and patterns of randomly placed objects

Point processes are natural building blocks for more complicated spatial processes such as patterns of random objects, for instance disks of random sizes. Let us consider a point process X and associate with each point X_i of X a random mark M_i, which could be the radius of a disk centered at X_i. By letting the mark be a vector with several components we could model more complex objects.

For the 2D gel electrophoresis images in Figures 9 and 10 we could associate with a protein at position $X_i = [X_{1i}X_{2i}]^T$ the mark $M_i = (S_i, C_i)$, where S_i is the expression level of the corresponding protein and C_i could describe the shape of the spot at X_i. A simple model would be to assume that the spot shape is a two-dimensional normal distribution with 2×2 covariance matrix C_i. The observed pixel gray level Y_x at a pixel with location x could then modeled by

$$Y_x = \sum_i S_i f(x, X_i, C_i) + \epsilon_x, \tag{75}$$

where ϵ_x is the observation noise at pixel x and

$$f(x, X_i, C_i) = \frac{1}{2\pi(\det C_i)^{1/2}} \exp(-\frac{1}{2}(x - X_i)^T C_i^{-1}(x - X_i)). \tag{76}$$

For the diffusing particles in Figures 14 and 15 we could consider a model

$$Y_x = \sum_i f(x, X_i, z_i) + \epsilon_x, \tag{77}$$

where again ϵ_x is the observation noise at pixel x, but the mark consists of the scalar z_i representing the vertical position of a particle relative to the focal plain. The function f could be assumed to be the same for all particles but needs to be estimated from data or by applying optical theory for the light scattering of the diffusing objects.

Similar models could be considered for the aerial photographs in Figures 2 and 4 where we could assume a similar shape for trees in a given view. This shape function could then be estimated from data combined with a simulation model based on the geometry and illumination of the trees from the sun (Larsen & Rudemo, 1998).

A specific problem is interaction between objects that overlap partly. In 2D gel electrophoresis it is natural to assume an additive model as in (75), but in the aerial photographs, and particularly for the diffusing particles, objects

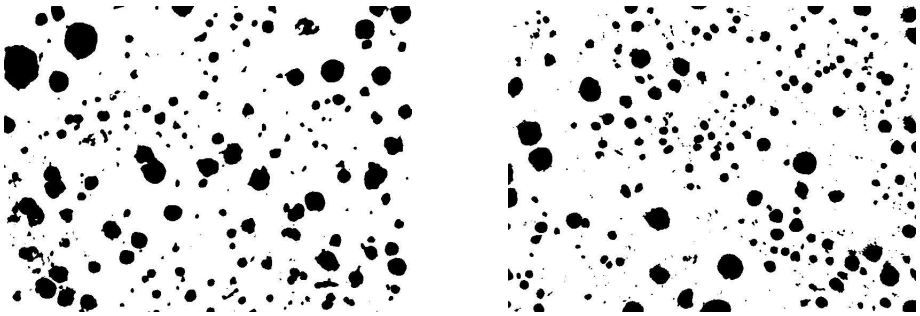

Figure 26: Binary images of two cuts in cast iron showing approximately disk-shaped defects. Data from Beretta (2000) and Månsson and Rudemo (2002).

may occlude each other and then an additive model may be an untenable approximation. In some applications such as the one shown in Figure 26 objects do not overlap.

Let us regard models for random placed disks. For disks of constant size we can then use the inhibition point process of Section 5.2 by placing disks of diameter d centered at the points of the thinned point process. In the following section we shall regard two modifications of this model.

6.1 Two processes of varying-sized disks

Let us regard marked point processes constructed in two steps as follows.

In the first step we generate a Poisson point process with constant intensity λ in the plane, and to each point in this point process we generate identically distributed radii with a *proposal* distribution function F_{pr}. The radii are independent mutually and of the point process.

In the second step we thin the generated point process by letting all pairs of points whose associated disks intersect 'compete'. A point is kept if it has higher weight in all pairwise comparisons, where the, possibly random, weights are assigned to the points according to two different approaches:
1) *Pairwise assignment of weights*: For each comparison, weights are assigned to the involved pair of points, and assignments are independent both within and between pairs.
2) *Global assignment of weights*: Weights are assigned once and for all to all points, and assignments to different points are independent. These weights are then used in all comparisons.

In both cases the weight of a point may depend on the associated radius. (When the weights are constant or deterministic functions of the radii, the two approaches coincide.)

It is possible to compute both the intensity of the point process after thinning and the radius distribution function after thinning. Details are given in Månsson and Rudemo (2002). Let us here only show a simulation example of disks before and after thinning with three different thinning procedure, see Figure 29.

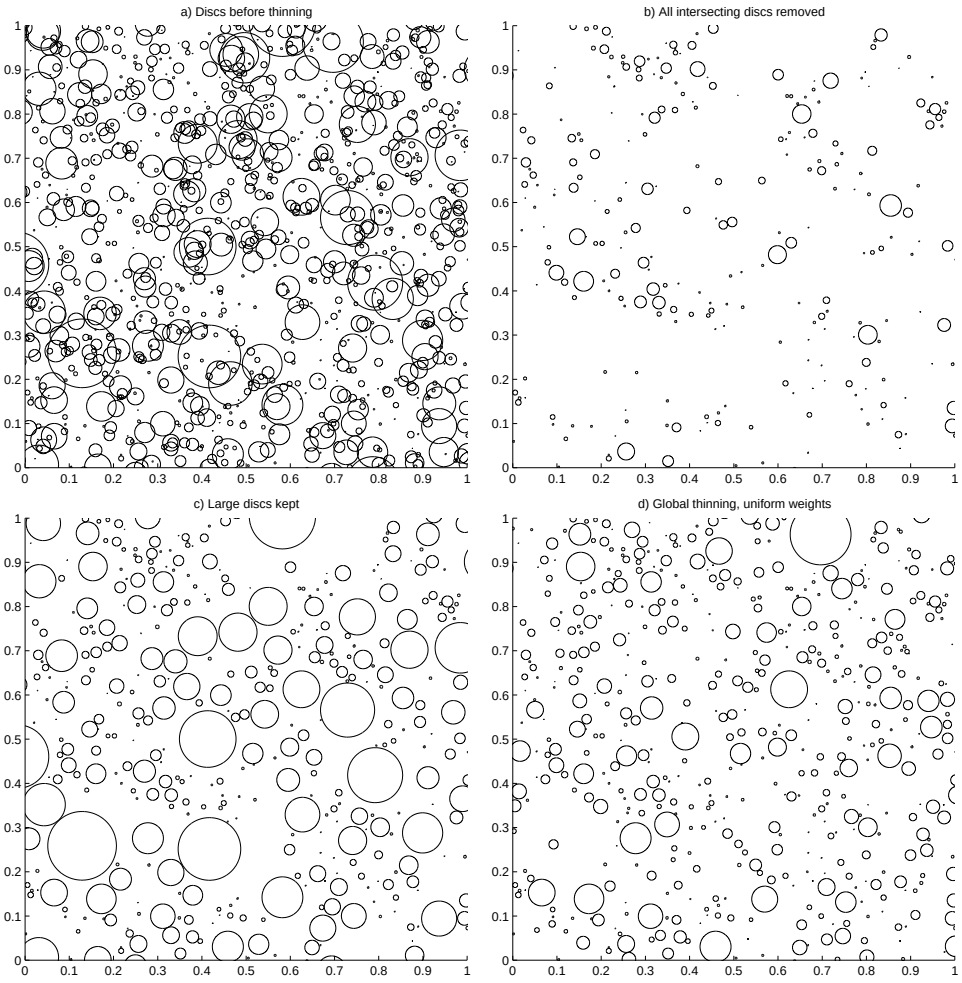

Figure 27: Simulation of a disk process before and after three different thinning procedures. In the first step a Poisson process with intensity 1000 in the unit square is generated with exponentially distributed disk radii with expectation 0.01.

7 Warping and matching

An important problem in analysis of multiple images is to match objects in different images. Thus we would like to know which spots in the 2D gel electrophoresis images in Figures 9 and 10 that correspond to each other, that is gauge the expression of the same protein. Similarly we want to match objects in Figures 14 and 15 in to order to be able to follow the diffusing particles and to estimate the diffusion coefficient of their motion. There is, however, a fundamental difference between these two problems. The diffusing particles move independently of each other except for the rare occasions when they come very close in all three dimensions. Thus displacements of particles that are close in the two-dimensional images are essentially independent of each other. In contrast, displacements of nearby spots in the electrophoresis images are highly correlated. The matching of objects in these two situations therefore demand quite different methods. In the present section we shall study warping methods which are useful for matching of objects in images such as the 2D gel images.

Suppose that we have a reference image $Y = Y(x)$ and another image Y' that we want to warp (transform) into Y as closely as possible according to some criterion by transforming locations such that $Y(x')$ is close to $Y(x)$. Here we regard x and x' as 2-dimensional column vectors and put

$$x' = f(x) \tag{78}$$

for some *warping function* f. For the affine warping function we have

$$x' = Ax + b = \begin{bmatrix} a_{11} & a_{12} \\ a_{21} & a_{22} \end{bmatrix} \begin{bmatrix} x_1 \\ x_2 \end{bmatrix} + \begin{bmatrix} b_1 \\ b_2 \end{bmatrix}. \tag{79}$$

A special case of the affine transformation is the Procrustes transformation for which

$$x' = \begin{bmatrix} c\cos\theta & c\sin\theta \\ -c\sin\theta & c\cos\theta \end{bmatrix} x + b. \tag{80}$$

A special case of the Procrustes transformation consists of a dilation (scale change with a fixed factor c) and a translation

$$x' = \begin{bmatrix} c & 0 \\ 0 & c \end{bmatrix} x + b = cx + b, \tag{81}$$

and another special case of the Procrustes transformation consists of a rotation and a translation,

$$x' = \begin{bmatrix} \cos\theta & \sin\theta \\ -\sin\theta & \cos\theta \end{bmatrix} x + b. \tag{82}$$

A simple nonlinear warping is the bilinear transformation

$$\begin{aligned} x_1' &= a_{11}x_1 + a_{12}x_2 + c_1x_1x_2 + b_1 \\ x_2' &= a_{21}x_1 + a_{22}x_2 + c_2x_1x_2 + b_2. \end{aligned} \tag{83}$$

We note that for fixed x_2 the bilinear transformation of x_1' is linear in x_1 (with slope and intercept depending on x_2) and, similarly, for fixed x_1 the transformation of x_2' is linear in x_2. This means that an axes-parallell rectangle in the x_1x_2-plane is transformed into a polygon with four corners in the $x_1'x_2'$-plane.

Another nonlinear warping function is the perspective transformation

$$\begin{aligned} x_1' &= (a_{11}x_1 + a_{12}x_2 + b_1)/(c_{11}x_1 + c_{12}x_2 + 1) \\ x_2' &= (a_{21}x_1 + a_{22}x_2 + b_2)/(c_{21}x_1 + c_{22}x_2 + 1). \end{aligned} \tag{84}$$

The perspective transformation may be used for matching the tree tops in Figures 2 and 4. Note that both the bilinear and the perspective transformations are generalisations of the affine transformation (79).

To choose parameters of a warping transformation $x' = f(x)$ we may consider a criterion function such as

$$L(Y', Y, f) = \sum_x (Y'(x') - Y(x))^2 + \lambda D(f) \tag{85}$$

where $D(f)$ is a distortion measure of the warping function f and λ is a constant determining the balance between closeness of matching and distortion. The distortion measure could for instance measure the deviation from linearity of the warping function, and could be a sum of squared second derivatives of f.

A useful type of warping consists af a net of locally bilinear transformation. This method is used in Glasbey and Mardia (2001) to warp images fish, haddock and whiting, see Figure 28, into each other. Similarly it is used in Gustafsson et al. (2002) to match 2D gel electrophoresis images such as those in Figures 9 and 10 into each other.

For reviews of image warping methods, see Glasbey and Mardia (1998, 2001).

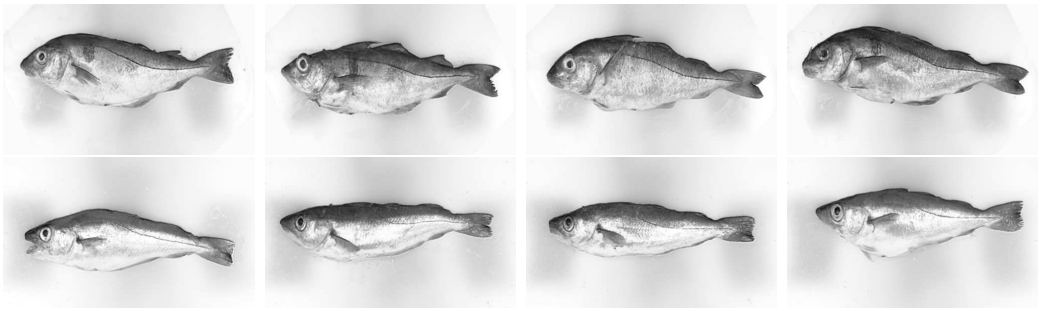

Figure 28: Images of fish warped into each other in Glasbey and Mardia (2001). Haddocks in the upper row and whitings in the lower row.